PHYSICAL REVIEW B VOLUME 4, NUMBER 12 15 DECEMBER 1971

Photoemission Investigation of Amorphous Germanium†

C. G. Ribbing,* D. T. Pierce, and W. E. Spicer
Stanford Electronics Laboratories, Stanford University, Stanford, California 94305
(Received 30 June 1971)

Photoemission measurements of amorphous germanium films have been made in the photon energy range 6.2–11.7 eV. A spectrum with one broad peak 1.25 eV below the high-energy cutoff is obtained, similar to earlier results of Spicer and Donovan. By comparison with gold spectra and using simple models for the resolution function and the high-energy edge in the electron distribution, the valence-band edge is placed 0.31 ± 0.05 eV below the Fermi energy, with no evidence for tailing of the density of states into the gap. Careful annealing measurements through several temperatures below the crystallization temperature showed no gradual changes until the rather abrupt appearance of crystalline structure after anneals to 300 and 350 °C. Deposition at rates of 2 and 26 Å/sec gave no significant change, nor did deposition onto substrates at −170–150 °C. The absolute photoelectric yield was measured, and its energy dependence found to be in very good agreement with recent theoretical results of Ballantyne. During successive annealings the yield first increased and then decreased to a significantly smaller value than the amorphous yield. A tentative explanation of this behavior is given within a random-network description of amorphous germanium.

I. INTRODUCTION

The electronic structure of amorphous germanium films has been intensively studied during recent years. Important contributions have been the theoretical work of Mott,[1,2] the optical and electrical measurements by Clark,[3] the optical studies of Tauc *et al.*,[4–6] the photoemission and optical measurements by Spicer and Donovan,[7–9] and the very recent studies of optical properties and their dependence on annealing and deposition rate by Theye.[10,11]

In the work reported here, which is an extension and refinement of the photoemission measurements of Spicer and Donovan, we particularly wanted to study how the annealing properties of amorphous Ge films varied with deposition conditions such as substrate temperature and evaporation rate. We also aimed to locate the Fermi level with respect to the valence-band edge. Since there has been considerable discussion[6] about tailing of the density of states into the gap, we also considered it worthwhile to repeat Spicer and Donovan's[9] comparison of photoelectron energy distribution curves (EDC's) for amorphous Ge with the EDC's of the same film annealed *in situ* until characteristic crystalline structure appeared.

II. EXPERIMENTAL

The measurements were performed with light monochromated to a full width at half-maximum of 0.10–0.20 eV over a photon energy range $6.2 \leq \hbar\omega \leq 11.8$ eV. The upper limit was set by the transmission cutoff of the LiF window on the ultrahigh-vacuum chamber. The photoelectron energy was measured with the retarding-field energy analyzer containing a spherical screened emitter, described by DeStefano and Pierce.[12,13] The energy distribution curves were obtained using the ac modulation technique reported by Spicer and Berglund[14] and by Eden.[15] The substrate holder was essentially a block of annealed copper which could be pivoted out of the collector so that the substrate was in a horizontal position for evaporation. The substrate was a polished disk-shaped single crystal of Ge (p type, 11 Ω cm, from semimetal). The substrate holder contained a heater and a thermocouple used to monitor the sample temperature.

A special cooling device was constructed which allowed the sample to be cooled to near liquid-nitrogen temperature. It consisted principally of a 15-cm-long 5-mm-thick flexible bundle of hydrogen-fired 0.013-mm oxygen-free high-conductivity (OFHC) copper wires, the ends of which were brazed into blocks of annealed copper. One block was tightly screwed onto the tip of a cold finger that could be filled with liquid nitrogen from outside of the chamber. The other end was connected to the substrate holder via a polished sapphire disk 1 mm thick, providing good thermal conduction to the substrate, but also electrical insulation from the chamber. An extra Pyrex washer had the effect of increasing the mechanical pressure between disk and substrate when the metal parts thermally contracted. This way of cooling does not give quite as low a final temperature as cooling the substrate directly with liquid nitrogen, but the extra noise due to the vibrations from the boiling liquid is avoided. A test showed that with this set up we could change the sample temperature from −170 to +600 °C both in the emission and evaporation positions.

After roughing, bake out, and pump down to ultrahigh vacuum, the substrate was heat cleaned at

more than 450 °C for about 15 min, and the e gun and source material were outgassed by preevaporation with the shutter closed. The evaporations were made with an e gun 48 cm from the substrate. The material used was intrinsic grade polycrystalline Ge obtained from Eagle-Picher. The rate of deposition and the final film thickness were monitored with a quartz microbalance mounted next to the substrate. All films studied in this work were about 1000 Å thick. During the evaporations the chamber base pressure of 1×10^{-10} Torr rose to 7×10^{-9} Torr for a deposition rate of 2 Å/sec. The higher deposition rate of 26 Å/sec increased the pressure to 1×10^{-7} Torr.

III. RESULTS AND DISCUSSION

Comparison to Previous Experiment

An EDC from a film evaporated onto a room-temperature (RT ≅ 293 °K) substrate at a rate of 2 Å/sec is compared in Fig. 1 to an EDC measured by Spicer and Donovan.[9] While there is general overall agreement, the two noticeable differences in our EDC are the 0.25-eV shift of the main peak to higher energy and the extra, very weak structure 3 eV below the main peak. We attribute the shift of the main peak to the improved resolution obtained using the screened-energy analyzer.[12] We locate the position of the main peak 1.25 eV below the valence-band edge. The new structure is too weak for us to conclude whether or not it is due to a real increase in the initial density of states. It appears just as probable that it originates from a superposition of scattered electrons onto the bottom of the valence band. This weak shoulder is visible through several photon energies, 10.2–11.7 eV, at about the same position relative to the main peak. When the measurements on this film were repeated at a sample temperature of −170 °C, a sharpening

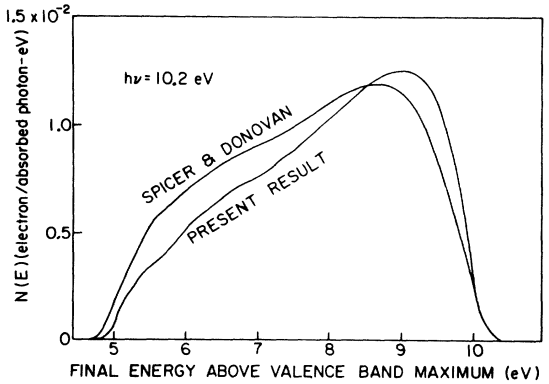

FIG. 1. A comparison of amorphous Ge EDC's of Spicer and Donovan (Ref. 9) and of the present work showing the 0.25-eV shift of the main peak and the extra low-energy structure 3 eV below the main peak.

of the leading edge of about 0.08 eV was observed at lower photon energies. We attribute this shift to a reduced electronphonon scattering.

Location of Valence-Band Edge

A difficult problem in photoemission studies of semiconductors is to place the high-energy cutoff properly, thereby locating the valence-band edge. The cutoff in the semiconductor is caused by the density of states and is not so steep as the metallic cutoff due to the Fermi function at RT. Also since the edge is broadened by the instrumental resolution function, it is necessary to somehow deconvolve the experimental curve to find the true cutoff in the density of states. (We shall use the concept of resolution function, meaning the experimental curve obtained from measuring an emitted δ-function distribution. Effectively, it is the same as the conventional "window" in ordinary spectroscopy, only with the opposite shift in nonsymmetric cases.)

In order to find the valence-band edge in amorphous Ge we have used the following procedure based on comparison with the cutoff for a metal. The EDC's of Au films were recorded in the same geometry and at the same low photon energies as the Ge films. Taking the metallic cutoff as the midpoint of the linear part of the high-energy edge gave a total width of the EDC which was in excellent agreement with the difference between the photon energy and work function of the collector as determined independently by a Fowler plot of the yield. Such a cutoff in the middle of the high-energy edge indicates that the resolution function is symmetric as can be seen from the idealized case in Figs. 2(a) and 2(b). A symmetric (case 1) and nonsymmetric (case 2) resolution function are shown in Fig. 2(a), where the arrows symbolize the emitted δ-function distribution of electrons. The nonsymmetric resolution of case 2 shifts the edge to lower energy and hence shifts the cutoff away from the middle of the linear region. Since imperfect analyzer geometry gives a nonsymmetric resolution function as in case 2, we suggest that this error is unimportant compared to random errors such as an unevenness in the analyzer work function and the spectral linewidth of the light. The principal reason for the insignificant geometrical error is probably the screened-emitter analyzer.

In order to get a quantitative description, the two simple models of a rectangular and triangluar resolution function are treated in Figs. 2(c)–2(f). The true emitted density of states in the metal is assumed to be broadened only by the Fermi function which we approximate by a straight edge like the dotted distribution in Fig. 2(c). This model neglects the curvature of the Fermi function close to 0 and 1, but since we are only going to use the straight middle part of the edges in our analysis we

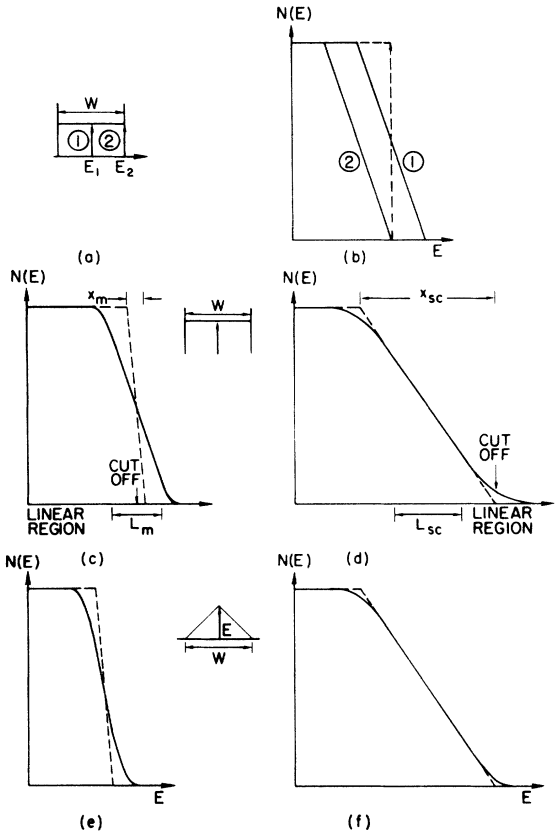

FIG. 2. Convolution of linear edges with model resolution functions: (a) symmetric and nonsymmetric rectangular resolution functions; (b) the effect of convolving a step-shaped edge with the resolution functions in (a) showing the shift of the edge in a nonsymmetric case; (c) "metallic" case, showing the convolution of a rectangular distribution function with a linear edge of smaller width; (d) "semiconductor" case, convolving a rectangular distribution function with a linear edge of larger width; (e) like (c) but with a triangular resolution function; (f) like (d) but with a triangular resolution function.

consider this to constitute a reasonable first approximation. By convolving[16] the rectangular resolution function with the true distribution (dotted line) we obtain the measured distribution (full line). The measured EDC will have a linear region with a corresponding interval L_m on the E axis. The relation, $L_m = W - x_m$, where W is the width of the resolution function and x_m the width of the true distribution, is easily found. To determine the instrumental constant W it remains to decide what width x_m should be attributed to the metallike distribution. This is done either by merely plotting the room-temperature Fermi function or by using the first-order expansion $f(E) = \frac{1}{2}[1 - (E - E_f)/2kT]$ and extrapolating to $f(E) = 0$ and 1. In both cases, at 20 °C a value of $x_m = 0.10$ eV ($\cong 4kT$) is obtained. L_m is determined from the measured Au EDC's to be 0.15 eV with good reproducibility through several low photon energies. We conclude from the Au measurements and from an analysis of these simple models that the resolution function is symmetric with a width $W = 0.25$ eV.

For comparison, the effect of a triangular window is shown in Fig. 2. The same over-all effect of this convolution is observed, i.e., rounding off corners and leaning the edge back. The rectangular resolution function was chosen for the analysis of the experimental results since it appears to give marginally better agreement with the experimental shape and is simpler to convolve.

A striking feature in the experimental EDC's from the amorphous Ge is that their leading edges also have a linear part. This indicates that the true distribution has a linear region of at least the same length. We take as the simple model for the semiconductor case a linear edge as represented by the dashed line in Fig. 2(d). The difference from the "metallic" edge is that the slope is considerably less steep and the true cutoff is at the end of the edge. Figure 2(d) shows the result of convolving this edge with the same resolution function as in Fig. 2(c). Two observations should be made. A large linear region is obtained in the middle of the edge and, as is to be expected when the resolution function has a smaller width than the measured structure, the slope of the edge is retained in that linear region. For the semiconductor, the relation between the linear edge and the width of the resolution function is $L_{sc} = x_{sc} - W$. The location of the true cutoff is $\frac{1}{2}W$ higher than the end of the linear region, which coincides with the extrapolation of the linear part to the E axis. It is not practical to relate anything to the cutoff of the instrumentally broadened EDC since the high-energy "foot" is disturbed by noise and zero line drift. Again for comparison, the effect of a triangular resolution function on the same edge is demonstrated in Fig. 2(f). This model appears to exaggerate the linearity of the experimental edge.

The application of the analysis above to recorded curves of Au and Ge is shown in Fig. 3. Average values of $L_{sc} = 0.29$ and $x_{sc} = 0\ 54$ eV are found. The valence-band edge is placed 0.31 ± 0.05 eV below the Fermi level by measurements from several EDC's at different low photon energies. The extrapolation of the linear part of the edge is in all cases in very close agreement to the cutoff obtained in this analysis, which shows the consistency of our simple models with the experimental results.

Results from Annealed Films

The amorphous films obtained by evaporation were all annealed in successive steps by raising the substrate temperature for about 1 h to a predetermined value and remaining at that temperature

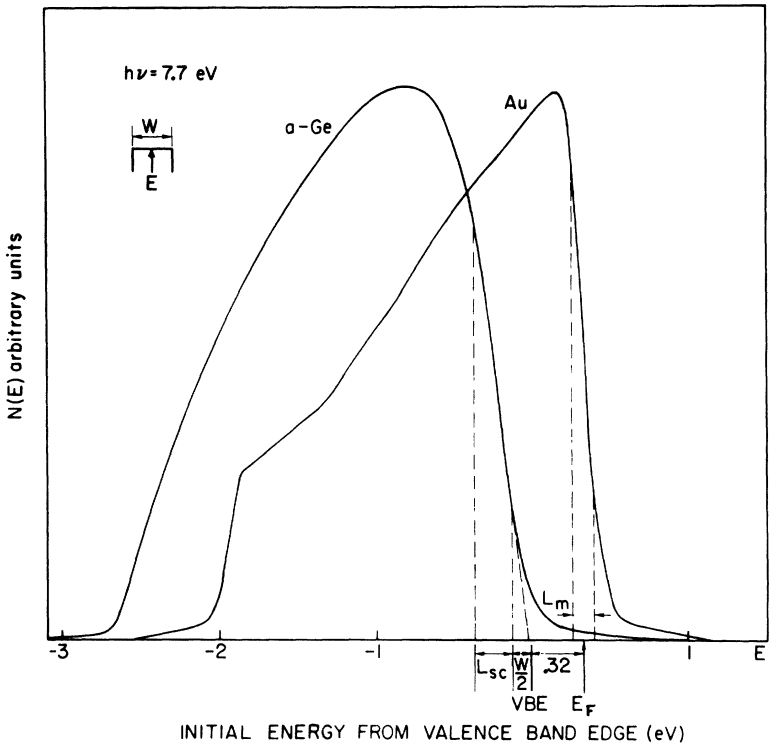

FIG. 3. Location of the valence-band edge of amorphous germanium using EDC's from Ge and Au recorded in the same geometry.

for half an hour. A precision of ± 5 °C was usual. The dramatic effect of heat treatment at 300 °C and above is demonstrated in Fig. 4. The broad structureless EDC of the amorphous material is transformed into the rich structure typical for crystalline Ge. After the final photoemission experiment it was furthermore verified by x-ray diffraction that the film gave (220) diffraction peaks that were not present on the other side of the (111)-oriented substrate. From the width of the diffraction peaks the size of the crystallites was estimated to be 200–300 Å.

Again the qualitative agreement with the annealing experiment of Spicer and Donovan[8] is satisfactory, but there is a shift in the crystallization temperature. Structure characteristic of crystalline film is apparent in our EDC's after annealing at 250–300 °C and is fully developed after annealing at 300–350 °C. The corresponding temperature intervals for the Ge films of Donovan and Spicer are 300–400 and 400–450 °C, resepctively, and the EDC's display a more gradual change. There still remains some uncertainty about the source of these differences. Adamski[17] has shown experimentally that the amorphous to polycrystalline and polycrystalline to epitaxial transformation temperatures are very sensitive to oxygen partial pressures as low as 5×10^{-9} Torr during evaporation. Nowick[18] also argues that the presence of any impurities that are insoluble in the cystalline phase stabilizes the amorphous phase. Crystallization would force such impurities to separate out in a second phase which corresponds to a high activation energy. The 1×10^{-11} Torr base pressure quoted by Spicer and Donovan is better than ours, so the only apparent sorce of extra oxygen in their experiment is their higher pressure during evaporation, 1×10^{-7}

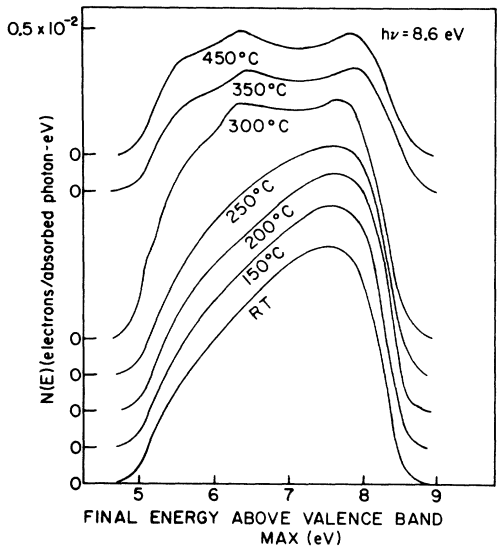

FIG. 4. The effect of annealing on the EDC's of amorphous Ge films. The curves are normalized to the absolute photoelectric yield.

Torr as compared to our 7×10^{-9} Torr. We note however that the poorer vacuum with the high evaporation rate discussed below did not effect the crystallization temperature. The preparation of the crystalline substrates, polishing and later heat cleaning in high vacuum, was virtually identical in both experiments so approximately the same amounts of substrate oxides were probably present initially.

As was originally noted by Spicer and Donovan the high-energy edge of the EDC's for amorphous Ge is at least as sharp as for polycrystalline Ge. In fact the crystalline edge is somewhat less steep, which can be understood as an effect of parabolic bands. It should be noted, however, that photoemission alone cannot rule out the possibility of a very small density of states in the gap $\sim10^{17}$ cm^{-3}, as reported by Tauc, Menth, and Wood[19] for amorphous As_2S_3.

A striking feature of Fig. 4 is the similarity between the EDC's from films heated only up to 250° C. This result is different from the recent results of Theye [10] who observes a gradual change in refractive index and absorption coefficient for annealing temperatures well below the crystallization temperature (400 °C). Thèye attributes this change to unsatisfied bonds which decrease in number when the film is annealed. We believe that these unsatisfied bonds are surface states on microvoids as demonstrated for amorphous Si by Moss and Graczyk.[20] Arguing against the presence of microvoids, Thèye claims that her films showed no decrease in density when annealed. A decrease, however, should only occur if the voids migrated to the surface, but not if they merely coalesced and thereby reduced the void surface and the number of "dangling bonds.'

Independent of what the defects are that cause the gradual changes upon annealing in Thèye's films, it seems as if they are not present in our films. A shift in the absorption edge of about 0.4 eV (Fig. 4, Ref. 10) would show up in the EDC's unless all the shift was due to a change in the final density of states below the vacuum level, an assumption that appears rather artificial. The obvious reason for the absence of defects should then be the several-orders-of-magnitude-lower base pressure in our case. Thèyes high deposition rate almost makes up for the quoted 10^{-6}-Torr evaporation pressure from the point of view of contamination. The fact that the crystallization temperature, however, was 100 °C higher than ours seems to indicate the presence of more impurities[17,18] as discussed above. The importance of Thèye's work therefore is that it demonstrates that it is possible by careful annealing to approach "the perfect amorphous state" obtainable directly in uhv. In view of these experiences it is tempting to speculate that the controversy[3,6,7,21] about tailing in the density of states into the forbidden gap is caused by different preparation techniques giving rise to more or less voids[22] in the film. The number of voids is substantially reduced if the film is deposited under clean conditions in ultrahigh vacuum.

Recently it has been noted by Donovan[23] and Spicer that Ge typically evaporates in the forms Ge_1, Ge_2, Ge_3, and Ge_4 and that the composition of the material striking the substrate could effect the characteristics of amorphous films so formed. One would expect the "perfect" amorphous film to be most closely approached when Ge arrives at the substrate as separated atoms. Low evaporation temperatures and long evaporation distances should maximize this since the fraction of atomic Ge is highest at low temperatures and since as the evaporation distance is increased, the probability of Ge_2, Ge_3, or Ge_4 breakup to produce more atomic Ge is increased. We did not check this hypothesis but we consider it to be a possible explanation for the discrepancies reported in the literature on the properties of amorphous germanium.

Effect of Substrate Temperatures

In subsequent evaporations the effect of different substrate temperatures was investigated. This is exemplified for the substrate temperatures – 170, 20, 150, and 260 °C in Fig. 5. The slight broadening of the 150 °C curve is most likely due to the fact that it was recorded with a conventional diode analyzer rather than with the screened-emitter analyzer. We find it a rather remarkable verification of the well-defined properties of amorphous Ge that the EDC's varied so little over a range in substrate temperature as large as 320 °C.

Apparently, the 260 °C substrate temperature was just as effective to crystallize the material as a 300 °C anneal. This is easy to understand, as pointed out by Nowick,[18] from the fact the mobility required for crystallization is easier to obtain on a free surface during an evaporation than in the already built-up film. The films evaporated at the three lower temperatures all crystallized in the same 250–350 °C range in contrast to the observation of Thèye [11] who reports a lower crystallization temperature the higher the substrate temperature. Tentatively, we suggest that this discrepancy is due to the larger amount of voids in Thèye's films The voids in the imperfect amorphous film impede crystallization, but they are reduced in number when the substrate is heated due to the higher surface mobility of the impinging atoms.

The object of the 260 °C evaporation was to see if the high-density form of amorphous Ge, reported by Donovan *et al.*,[22] had some characteristic feature in photoemission. Due to the lower crystallization temperature this question remains to be answered. In principle the high-density phase could have been formed on the 150 °C substrate,

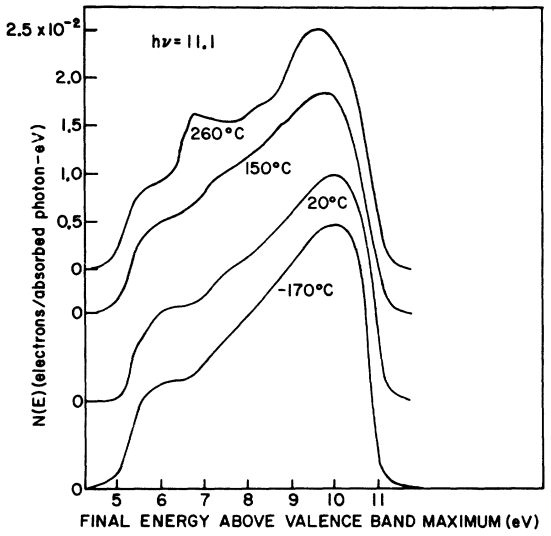

FIG. 5. The effect of different substrate temperature on the EDC's of Ge films. The 150 °C curve was recorded with a conventional diode analyzer.

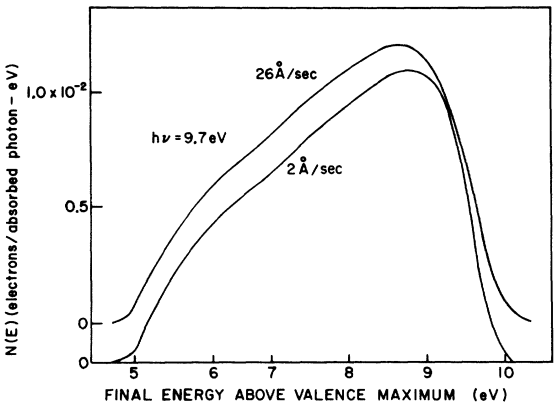

FIG. 6. Two normalized EDC's of Ge films deposited on RT substrate at different rates.

but in such a case the same EDC's were obtained as in the case of the normal-density amorphous film.

Effect of Rate of Deposition

To investigate what influence the evaporation rate could have on the EDC's of amorphous Ge, one evaporation was tried with as high a rate as was possible within the constraints of the long source-to-substrate distance and the desire to maintain a pressure $\leq 1\times10^{-7}$ Torr. A rate of 26 Å/sec was recorded. This is far from the 200 Å/sec reported by Thèye,[10,11] but it was hoped that any gross effect of deposition rate would be revealed by the increase from 2 to 26 Å/sec. A pressure of 1×10^{-7} Torr during an evaporation of more than 30 sec corresponds to a maximum contamination of 1 to 2 monolayers of gas molecules over the 1000 Å of the film. Therefore, it is not conclusively demonstrated that the shift to lower energy of the main peak and the broadening of the high-energy edge in Fig. 6 really stems from the high evaporation rate. The possibility of contamination cannot be ruled out.

Photoelectric Yield

The yield of photoemitted electrons per incident photon was measured over the entire energy range using a calibrated Cs_3Sb photocell[24] and a +45 V bias on the collector. The absolute yield was calculated using the formula $Y=y/(1-R)T$, where y is the yield found from measurement, R is the reflectivity of the film, and T is the transmission of the LiF window. Since no reflectivity data for fine grain polycrystalline films were available we chose to use reflectivity data for amorphous Ge.

The resulting yields for amorphous and annealed film are presented in Fig. 7. At high energies the yield of the amorphous film is between the yield of the film annealed at 300 and 450 °C. We believe that this surprising result can be interpreted in the following way. Assuming that our amorphous Ge forms an ideal or almost ideal tetrahedral random network,[25] it is easily conceived that the thermal scattering is higher than in a single crystal with

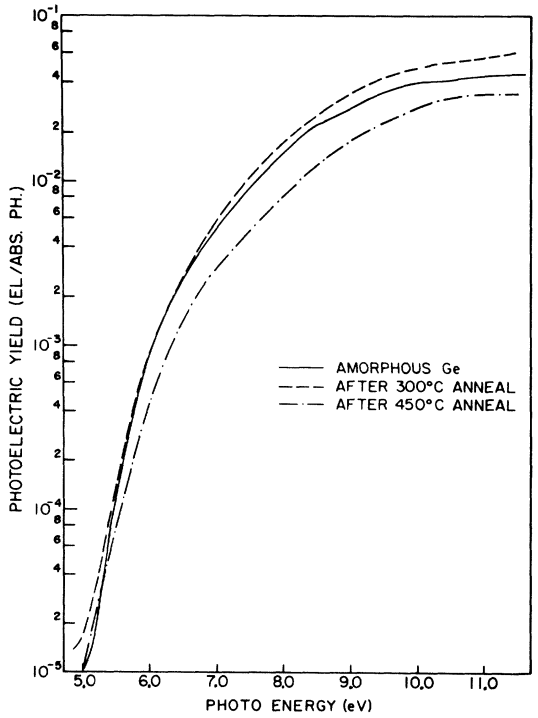

FIG. 7. The absolute photoelectric yield for an as deposited Ge film, after a 300 °C anneal and after a 450 °C anneal.

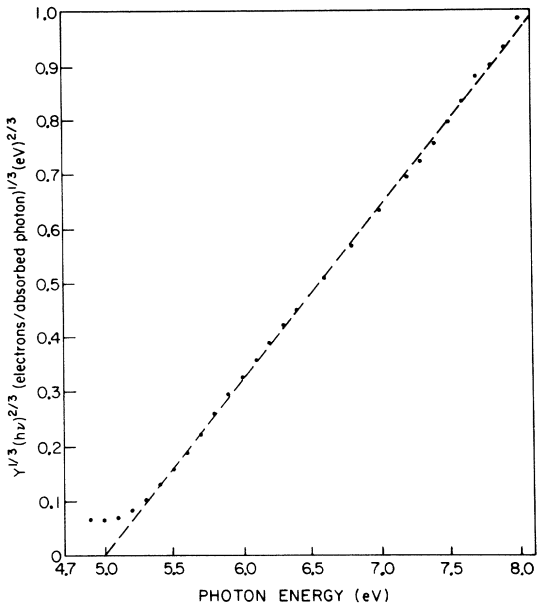

FIG. 8. The photoelectric yield of amorphous Ge fitted to the relation of Ref. 28.

long-range order. This will give the amorphous film a higher yield since increased probability of elastic or almost elastic scattering will increase the probability that an excited electron reaches the escape cone.[26] This argument is based on the assumption that the electron-electron scattering length is larger than the defect scattering length. The first annealing step to 300 °C can then be understood as breaking up the network and creating small crystallites ($\ll 200$ Å). The large amount of internal surface barriers will *increase* the total scattering giving rise to the higher yield obtained. Continued annealing to 350–450 °C increases the grain size which will reduce the scattering and thus the yield in complete qualitative agreement with the results in Fig. 7. The choice of amorphous reflectivity data cannot be responsible for this effect, since reflectance values reported[27] for crystalline Ge would make the yield for the 450 °C annealed film even lower by as much as 25% at 11 eV. It could, however, make the difference between the amorphous and the 300 °C annealed film much smaller. It can be remarked that this behavior of the yield through annealing would be very difficult to reconcile with any kind of microcrystalline model where the annealing process has to be conceived as a successive growth of microcrystallites.

Attempts to fit the energy dependence of the yield for the amorphous film to any simple power law[28] failed, even for energy ranges close to threshold. Very recent results of Ballantyne,[29] however, gave a remarkably good fit over a range of almost 3 eV as seen in Fig. 8. The energy dependence of the yield derived by Ballantyne for the case of a rectangular energy distribution of excited electrons is $Y \propto (h\nu - \varphi)^3/(h\nu)^2$, where $h\nu$ is the photon energy and φ is the threshold. The derivation of this formula includes a smearing out of the rectangular distribution by a phenomenological scattering against phonons, defects, impurities, or surfaces. The extrapolated value for the threshold is found to be 4.98 ± 0.04 eV, in good agreement with the sum of the values for the work function 4.63 ± 0.04 eV and the difference in energy between Fermi level and valence-band maximum 0.31 ± 0.05 eV that were obtained from the EDC's.

ACKNOWLEDGMENTS

We would like to thank Professor J. M. Ballantyne for giving us access to his results prior to publication and for several valuable comments. We would like to thank Dr. T. Donovan for providing the reflectivity data for amorphous germanium as well as for several informative discussions. We also want to express our appreciation of the endurance and skill displayed by Phil McKernan in constructing the cooling device.

---

†Work supported by the Advanced Projects Agency through the Army Office of Scientific Research and through the Center for Material Science at Stanford University.

*On a grant from the Swedish Board for Technical Development.

[1]N. F. Mott, Advan. Phys. 16, 49 (1967).

[2]N. F. Mott, Phil. Mag. 19, 835 (1968).

[3]A. H. Clark, Phys. Rev. 154, 750 (1967).

[4]J. Tauc, R. Grigrovici, and A. Vancu, Phys. Status Solidi 15, 627 (1966).

[5]J. Tauc, Mater. Res. Bull. 3, 37 (1968).

[6]J. Tauc, A. Abraham, R. Zallen, and M. Slade, J. Non-Cryst. Solids 4, 279 (1970).

[7]T. M. Donovan and W. E. Spicer, Phys. Rev. Letters 22, 20 (1969); 22, 1058 (1969).

[8]W. E. Spicer and T. M. Donovan, Phys. Rev. Letters 24, 11 (1970); 24, 595 (1970).

[9]W. E. Spicer and T. M. Donovan, J. Non-Cryst. Solids 2, 66 (1970).

[10]M. L. Thèye, Mater. Res. Bull. 6, 2 (1971); 6, 103 (1971).

[11]M. L. Thèye, Opt. Commun. 2, 329 (1970).

[12]T. DiStefano and D. Pierce, Rev. Sci. Instr. 41, 180 (1970).

[13]D. Pierce and T. DiStefano, Rev. Sci. Instr. 41, 1740 (1970).

[14]W. E. Spicer and C. N. Berglund, Rev. Sci. Instr. 35, 1665 (1964).

[15]R. C. Eden, Rev. Sci. Instr. 41, 252 (1970).

[16]E. A. Guillemin, *Theory of Linear Physical Systems* (Wiley, New York, 1963), Chap. 13.

[17]R. F. Adamsky, J. Appl. Phys. 40, 4301 (1969).

[18]A. S. Nowick, Comments Solid State Phys. V2, 155

(1970).
[19]J. Tauc, A. Menth, and D. L. Wood, Phys. Rev. Letters 25, 749 (1970).
[20]S. C. Moss and J. F. Graczyk, Phys. Rev. Letters 23, 1167 (1969).
[21]J. W. Osmun and H. Fritzsche, Appl. Phys. Letters 16, 87 (1970).
[23]T. Donovan (private communication).
[22]T. M. Donovan, E. J. Ashley, and W. Spicer, Phys. Letters 32A, 85 (1970).
[24]R. Y. Koyama, thesis, Technical Report No. 5223-1, Appendix 1 (Stanford University, (1969) (unpublished).
[25]D. E. Polk, J. Non-Cryst. Solids 5, 365 (1971).
[26]R. N. Stuart and F. Wooten, Phys. Rev. 156, 364 (1967).
[27]H. R. Philipp and H. Ehrenreich, Phys. Rev. 129, 1550 (1963).
[28]E. O. Kane, Phys. Rev. 127, 131 (1962).
[29]J. Ballantyne, Phys. Rev. (to be published).

PHYSICAL REVIEW B VOLUME 4, NUMBER 12 15 DECEMBER 1971

Excitonic Theory of Electroabsorption: Phonon-Assisted Indirect Transitions in Si and Ge†

Binneg Y. Lao,* John D. Dow, and Frank C. Weinstein‡
Joseph Henry Laboratories of Physics, Princeton University, Princeton, New Jersey 08540
(Received 9 July 1971)

The theory of indirect phonon-assisted optical absorption by semiconductors in a uniform electric field is developed with particular attention being paid to the effects of electron-hole correlations (excitons). The Coulombic electron-hole interaction is treated within the Wannier-exciton effective-mass approximation. The physics of indirect electroabsorption is discussed, and it is found that exciton theory predicts an indirect absorption spectrum which is dramatically different, both qualitatively and quantitatively, from the spectrum predicted by one-electron theory (neglecting electron-hole correlations). The excitonic correlations are responsible for four qualitative features found in measured differential electroabsorption spectra but omitted by the one-electron theory: (i) The threshold for optical absorption by excitons lies at a lower energy; (ii) excitons cause a sharp drop on the high-energy side of the first differential electroabsorption peak; (iii) the amplitude of the differential absorption is enhanced by excitons; and (iv) excitonic spectra exhibit longer periods of spectral oscillations. These excitonic effects are analogous to effects previously predicted for direct transitions. Numerical calculations of the differential electroabsorption at the indirect edges of Ge and Si are compared with the data of Frova *et al.* and are found to be in excellent agreement with experiment.

I. INTRODUCTION

In recent years, modulation spectroscopy[1] has become one of the most powerful tools for probing the electronic states of solids. In the area of electric field modulation experiments, in which the spectra are obtained by measuring the response of a semiconducting solid to an external square-wave-modulated electric field, differential absorption measurements have been reported for both direct- and indirect-band-gap semiconductors.[2] Until recently, the theoretical treatments of electroabsorption data have been limited to the one-electron approximation,[3] which neglects the excitonic correlations between the positions of the optical electron and hole. These correlations, caused by the final-state Coulomb interaction between the electron and the hole, lead to the formation of bound and continuum states of the exciton, and significantly change the shape of absorption spectra from that predicted by one-electron theory.

The importance of the final-state interactions on measured spectra was recognized several years ago,[2] but the theory of electroabsorption has only recently become sufficiently sophisticated[4-6] to evaluate these correlation effects. In this paper we report the first calculations[7] to go beyond the one-electron approximation and to include electron-hole correlations in the evaluation of the differential electroabsorption coefficient at an indirect edge. We use these results to analyze the indirect electroabsorption data for Ge and Si measured by Frova, Handler, Germano, and Aspnes.[2]

One purpose of these calculations is to test the validity of the Elliott theory[8] of absorption by excitons in indirect phonon-assisted optical transitions. Such transitions in Ge and Si represent an ideal test of the theory because (i) energy conservation forbids many of the broadening processes that tend to complicate the spectra at higher optical thresholds, (ii) the energy-band structures are well known for these materials,[9] and (iii) the absorption coefficient is sufficiently small to guarantee that most of the absorption occurs in the